DNA Binding of Δ- and Λ-[Ru(phen)$_2$DPPZ]$^{2+}$

Catharina Hiort, Per Lincoln,* and Bengt Nordén

Contribution from the Department of Physical Chemistry, Chalmers University of Technology, S-412 96 Gothenburg, Sweden

Received October 29, 1992

Abstract: Linear dichroism (LD) spectroscopy and steady-state as well as time-resolved luminescence spectroscopy have been used to investigate the interaction of the Δ and Λ enantiomers of Ru(phen)$_2$DPPZ^{2+} (phen = 1,10-phenanthroline; DPPZ = dipyrido[3,2-*a*:2′,3′-*c*]phenazine) with DNA. The pure enantiomers, which were difficult to separate by traditional resolving methods, were synthesized via a chiral precursor. Changes in luminescence, isotropic absorption and excited state lifetimes upon binding, and the LD observed in flow-oriented DNA systems provide detailed information about the DNA binding of the enantiomers. Flow LD shows that both enantiomers bind to DNA in a well-defined manner with an orientation of the dipyridophenazine chromophore consistent with intercalation of this moiety between base-pairs. Both enantiomers are found to show luminescence in the presence of DNA to which they bind very strongly ($K \approx 10^8$ M^{-1}); however, the relative luminescence quantum yield of the bound Δ enantiomer is 6–10 times larger than that of the bound Λ enantiomer. Furthermore, for each enantiomer two distinct excited state lifetimes are found in varying proportions depending on the binding ratio. The large difference in luminescence quantum yield between the enantiomers is interpreted in terms of slightly different intercalation geometries of the dipyridophenazine ligand, resulting in different protections from quenching by solvent water and diastereomeric differences in the interactions between enantiomers bound in contigue on DNA.

Introduction

The mixed-ligand complexes [Ru(phen)$_2$DPPZ]$^{2+}$ (Figure 1)[1] and [Ru(bipy)$_2$DPPZ]$^{2+}$ have been proposed as luminescent DNA probes on the basis of their strong binding to double helical DNA and a practically negligible background emission of any unbound complex.[2] In organic solvents and micelles, as well as when bound to DNA, [Ru(bipy)$_2$DPPZ]$^{2+}$ displays luminescence, although it is completely quenched for the free complex in aqueous solution.[2-4] The quantum yield in aqueous buffer is increased by a factor >10^4 in the presence of DNA to which the complex binds with an equilibrium binding constant >10^6 M^{-1} in 50 mM NaCl buffer.[2a] Based on evidence for unwinding and considering the extended planar structure of the DPPZ ligand an intercalative binding mode for the complex has been proposed.[2a] This conclusion has some support in luminescence polarization data showing that the complex is highly immobilized on DNA.[2c]

Previous studies on [RuL$_2$DPPZ]$^{2+}$ complexes have been on racemates, although it is known that interaction of DNA with chiral metal complexes, such as tris(1,10-phenanthroline)-ruthenium(II) and related compounds, is in general enantioselective.[2c,5,6] Conventional resolving methods based on formation of diastereomeric salts failed in our laboratory with [Ru-(phen)$_2$DPPZ]$^{2+}$. However, we here report a high-yield synthesis of enantiomerically pure Δ- and Λ-[Ru(phen)$_2$DPPZ]$^{2+}$ by condensation of 1,2-diaminobenzene with the readily resolvable enantiomers of bis(1,10-phenanthroline)(1,10-phenanthroline-5,6-dione)ruthenium(II). In addition, this chiral intermediate dione complex, by condensation with suitable aromatic ortho diamines, could provide access to pure enantiomers of analogues of [Ru(phen)$_2$DPPZ]$^{2+}$. Luminescence, excited state lifetimes, isotropic absorption, and linear dichroism data are reported for the interaction of calf thymus DNA with Δ- and Λ-[Ru-(phen)$_2$DPPZ]$^{2+}$ in order to obtain detailed information about the binding of the respective complexes. Our results show that opposite enantiomers bind to DNA with comparable binding strengths ($K_{eff} \approx 10^8$ M^{-1}) but that the relative quantum yield of the bound Δ complex is some 6–10 times higher than that of the bound Λ complex. This means that more than 85% of the emission observed for racemic [Ru(phen)$_2$DPPZ]$^{2+}$ bound to DNA emanates from the Δ enantiomer. Flow linear dichroism results show that the binding geometries of the two enantiomers to DNA are similar and unaltered over a wide range of binding ratios. The negative linear dichroism of the DPPZ-ligand transition at 380 nm supports a binding model in which both enantiomers of [Ru(phen)$_2$DPPZ]$^{2+}$ bind to DNA by intercalation with the DPPZ chelate wing inserted between base pairs, as suggested by Friedman et al.[2a] Two distinct luminescence lifetimes are found to be present for each enantiomer when bound to calf thymus DNA as well as to [poly(dG-dC)]$_2$ and [poly-(dA-dT)]$_2$. For both enantiomers the longer lifetime fraction is found to increase with binding ratio. We propose here that it is

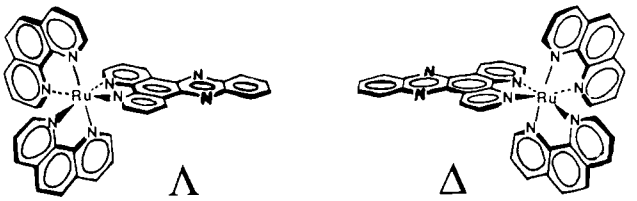

Figure 1. Absolute configurations of the Λ and Δ enantiomers of [Ru-(phen)$_2$DPPZ]$^{2+}$.

(1) DPPZ = dipyrido[3,2-*a*:2′,3′-*c*]phenazine, phen = 1,10-phenanthroline, bipy = 2,2′-bipyridyl, L = ligand (phen or bipy).

(2) (a) Friedman, A. E.; Chambron, J.-C.; Sauvage, J.-P.; Turro, N. J.; Barton, J. K. *J. Am. Chem. Soc.* **1990**, *112*, 4960. (b) Friedman, A. E.; Turro, N. J.; Barton, J. K. *Abstract for the Fifth International Conference on Bioinorganic Chemistry (ICBIC-5)*, August 4–10, Oxford, U.K., 1991; p 442. (c) Friedman, A. E.; Kumar, C. V.; Turro, N. J.; Barton, J. K *Nucleic Acids Res.* **1991**, *19(10)*, 2595. (d) Hiort, C.; Lincoln, P.; Eriksson, M.; Nordén, B. *Molecule Aspects of the Sequence-Specific Binding of Metal Compounds to Nucleic Acids. Workshop of the Royal Netherlands Academy of Arts and Sciences*, December 10–13, Harlem: The Netherlands, 1991; p 8.

(3) (a) Chambron, J.-C.; Sauvage, J.-P.; Amouyal, E.; Koffi, P. *New J. Chem.* **1985**, *9*, 527. (b) Amouyal, E.; Homsi, A.; Chambron, J.-C.; Sauvage, J.-P. *Chem. Soc. Dalton Trans.* **1990**, 1841.

(4) Chambron, J.-C.; Sauvage, J.-P. *Chem. Phys. Lett.* **1991**, *182* (6), 603.

(5) (a) Nordén, B.; Tjerneld, F. *FEBS Lett.* **1976**, *67*, 368. (b) Kumar, C. V.; Barton, J. K.; Turro, N. J. *J. Am. Chem. Soc.* **1985**, *107*, 5518. (c) Barton, J. K.; Goldberg, J. M.; Kumar, C. V.; Turro, N. J. *J. Am. Chem. Soc.* **1986**, *108*, 2081. (d) Satyanarayana, S.; Dabrowiak, J. C.; Chaires, J. B. *Biochemistry* **1992**, *31*, 9319.

(6) (a) Hiort, C.; Nordén, B.; Rodger, A. *J. Am. Chem. Soc.* **1990**, *112*, 1971. (b) Eriksson, M.; Leijon, M.; Hiort, C.; Nordén, B.; Gräslund, A. *J. Am. Chem. Soc.* **1992**, *114*, 4933.

0002-7863/93/1515-3448$04.00/0

the distribution of intercalated complexes along the DNA molecule that is the origin of the two lifetimes in such a way that complexes bound in contigue have longer lifetime. The intercalative binding geometry and the high DNA binding affinity of [Ru(phen)$_2$(DPPZ)]$^{2+}$ are characteristics that contrast the behavior of the parent compound [Ru(phen)$_3$]$^{2+}$, which shows a comparatively weak binding to DNA. Various binding models have been proposed for [Ru(phen)$_3$]$^{2+}$,[5] including intercalation;[5b,c] however, more recent investigations indicate that this complex binds non-intercalactively to DNA.[6,5d]

Experimental Section

Chemicals. Calf thymus DNA was purchased from Sigma and double-stranded poly(dG-dC) and poly(dA-dT) (average lengths > 500 bp) from Pharmacia Biochemicals. Organic solvents and other chemicals were obtained commercially and used as received, except for 1,2-diaminobenzene which was recrystallized from water prior to use. Calf thymus DNA was long enough to give good flow orientation, while the synthetic polynucleotides had contour lengths that were insufficient to give reliable linear dichroism data for the associated metal complexes. The concentrations of calf thymus DNA, [poly(dA-dT)]$_2$, and [poly(dG-dC)]$_2$ were determined spectrophotometrically using the molar absorptivities 6600 (258 nm), 6600 (262 nm), and 8400 (254 nm) M^{-1} cm^{-1}, respectively.[7-9] All DNA and polynucleotide solutions were prepared in buffer containing 10 mM NaCl and 1 mM sodium cacodylate, adjusted to pH 7, in deionized triply filtered water (Millipore). Literature methods were used for preparation of bis(1,10-phenanthroline)dichlororuthenium(II)[10] and of the sodium salts of the enantiomers of arsenyltartaric acid.[11] 1,10-Phenanthroline-5,6-dione (1,10-phenanthrolinequinone) has been prepared from phenanthroline by a multistep synthesis via 5-nitrophenanthroline (15% yield)[12] or by a one-pot oxidation (20% yield).[3b] We found that better yields (45%) could be obtained by the oxidation of phenanthroline with a mixture of sulfuric and nitric acid in the presence of bromine, as originally described by Gillard et al. for the oxidation of [Co(phen)$_3$]$^{3+}$ to the corresponding tris(dione) complex.[13] Racemic bis-(1,10-phenanthroline)(1,10-phenanthroline-5,6-dione)ruthenium bis-(hexafluorophosphate) was prepared from 1,10-phenanthroline-5,6-dione and bis(1,10-phenanthroline)dichlororuthenium(II) analogously to the procedure for the corresponding bis(2,2'-bipyridyl) complex[14] and recrystallized from acetonitrile/diethyl ether. Metal complex stock solutions, prepared by dissolving the chloride salts in buffer, were kept in the dark to avoid photodegradation.

1,10-Phenanthroline-5,6-dione. 1,10-Phenanthroline (5.00 g) was dissolved in portions during stirring in 30 mL of concentrated sulfuric acid in a 100-mL round-bottom flask equipped with a reflux condenser. Sodium bromide (2.50 g) was then added, followed by 15 mL of 70% nitric acid. The mixture was heated to boiling and then kept refluxing for 40 min. Heating was then reduced and the reflux condenser removed to allow the bromine vapors to escape during 15 min of gentle boiling. After being cooled the mixture was poured onto 400 g of ice, carefully neutralized to pH 7 with about 150 mL of 10 M sodium hydroxide, and allowed to stand for 30 min. The turbid solution was filtered, and the solids were extracted with 100 mL of boiling water. The insoluble material was removed from the cooled extract by filtration, and the combined aqueous solutions were extracted with 5 × 100 mL dichloromethane. The organic phase was washed with 50 mL of water, dried over anhydrous sodium sulfate, and evaporated under reduced pressure. The crystalline residue was recrystallized from 400 mL of toluene to give the dione: 2.64 g (45%), yellow-orange needles, mp 257 °C (lit. mp 258 °C[12]).

Δ- and Λ-Bis(1,10-phenanthroline)(1,10-phenanthroline-5,6-dione)-ruthenium Bis(hexafluorophosphate). The chloride salt of the compound was precipitated from a solution of 0.50 g of the racemic hexafluorophosphate in 10 mL of acetone by the addition of an acetone solution of tetra-*n*-butylammonium chloride. The solids were filtered off, washed with acetone and diethyl ether, dried, and dissolved in 20 mL of water. The filtered solution of the racemic chloride was then heated to boiling and 1.0 g of sodium arsenyl-L(+)-tartrate, dissolved in 5 mL of hot water, was added. Crystallization of the Λ-arsenyl-L(+)-tartrate diastereomer, initiated by scratching with a glass rod, was allowed to proceed overnight with slow cooling to 4 °C. The brown crystals were removed by filtration and washed with ice-cold water. The Δ-enriched hexafluorophosphate was obtained from the mother liquor by precipitation with aqueous ammonium hexafluorophosphate, converted to the chloride form, and treated with sodium arsenyl-D(−)-tartrate as described above.

For purification each enantiomeric salt with arsenyltartrate was dissolved in 5 mL of hot dimethyl sulfoxide and filtered. The filtrate was diluted with 15 mL of boiling water before 2 mL of a hot aqueous solution of 0.2 g of the appropriate sodium arsenyltartrate enantiomer was added.

Crystallization was initiated by scratching and the mixture was slowly cooled overnight. Each recrystallized sample was dissolved in 20 mL of hot 20% acetic acid and the filtered solutions were precipitated with an ammonium hexafluorophosphate solution. The precipitates were collected on a filter, washed with water, and recrystallized from acetone/water to give the Δ enantiomer (0.12 g, 48%) and the Λ enantiomer (0.16 g, 64%) as brown-black crystals.

Δ- and Λ-Bis(1,10-phenanthroline)(dipyrido[3,2-*a*:2',3'-*c*]phenazine)-ruthenium Bis(hexafluorophosphate). The dione complex (96 mg, 0.1 mmol) and 43 mg (0.4 mmol) of 1,2-diaminobenzene were dissolved in 1 mL of acetonitrile in a small screwcapped vial and heated on a boiling water bath for 45 min. After the mixture was cooled, the product was precipitated with a large excess of diethyl ether. The precipitate was filtered off, recrystallized by slow evaporation of an acetone/water solution, and dried for 12 h at 60 °C to give the DPPZ complex: 53 mg (51%) of dark red crystals.[15] Halide salts were prepared from the hexafluorophosphates by precipitation in acetone solution with the appropriate tetra-*n*-butylammonium halide. Anal. Calcd for Ru(phen)$_2$(DPPZ)(PF$_6$)$_2$·1.5H$_2$O: C, 47.53; H, 2.75; N, 10.56. Found (Λ): C, 47.6; H, 2.5; N, 10.3. Found (Δ): C, 48.1; H, 2.5; N, 10.4. UV/vis (Λ in water; λ_{max} in nm, $\epsilon/10^3$ M^{-1} cm^{-1} enclosed in parentheses): 439 (20), 372 (21.8), 263 (117). CD (Λ in water; λ_{extr} in nm, $\Delta\epsilon$/M^{-1} cm^{-1} enclosed in parentheses): 465 (+17), 416 (−18), 315 (+42), 301 (+66), 267 (+363), 254 (−178). ^{1}H NMR (Λ as dibromide, 400 MHz, CD_2Cl_2): δ 9.64 (dd, 2 H), 8.51 (m, 4 H), 8.47 (d, 2 H), 8.41 (m, 2 H), 8.37 (dd, 2 H), 8.25 (d, 2 H), 8.15 (s, 4 H), 8.02 (m, 2 H), 7.90 (dd, 2 H), 7.79 (m, 4 H).

The ^{1}H NMR spectrum of the Λ enantiomer confirmed the structure and showed no significant impurities. The enantiomeric purity was determined by employing the chiral shift reagent europium(III) tris(3-trifluoroacetyl-*d*-camphorate).[16] The analysis was calibrated by adding 5% of the Δ enantiomer to the sample. It was found that the Λ preparation contained less than 1% Δ enantiomer. Comparison of circular dichroism spectra (relative to absorption intensities) established the same (±1%) high optical purity for the Δ enantiomer.

Luminescence and Absorption Measurements. Steady state luminescence measurements were carried out using an Aminco SPF-500 spectrofluorometer in the quanta correction mode on air-saturated solutions at ambient temperature. The emission intensities at 610 nm were measured upon excitation at 440 nm in the charge-transfer absorption band of the metal complex. The intensity values were corrected for the absorption of excitation light according to the Bouguer–Lambert–Beer law:

$$I_{corr} = I_{meas} \times 10^{0.63A} \quad (1)$$

where A is the absorbance of the sample at the excitation wavelength, measured in a 1-cm cell, and 0.63 cm is an effective path length for the exciting light in the 1 × 1 cm luminescence cell in the optics of the particular fluorimeter (determined empirically as an instrument constant).[17c] Luminescence lifetimes were determined with single-photon

(7) Felsenfeld, G.; Hirschman, S. Z. *J. Mol. Biol.* **1965**, *13*, 409.
(8) Wells, R. D.; Larson, J. E.; Grant, R. C.; Shortle, B. E.; Cantor, C. E. *J. Mol. Biol.* **1970**, *54*, 465.
(9) Inman, R. B.; Baldwin, R. L. *J. Mol. Biol.* **1962**, *5*, 172.
(10) Giordano, P. J.; Bock, C. R.; Wrighton, M. S. *J. Am. Chem. Soc.* **1978**, *100*, 6960.
(11) Trifonov, A.; Elenkowa, N. *Z. Phys. Chemie (Leipzig)* **1955**, *205*, 124.
(12) Dickeson, J. E.; Summers, L. A. *Aust. J. Chem.* **1970**, *23*, 1023.
(13) Gillard, R. D.; Hill, R. E. E.; Maskill, R. *J. Chem. Soc. A* **1970**, 1447.
(14) Goss, C. A.; Abruna, H. D. *Inorg. Chem.* **1985**, *24*, 263.
(15) Samples for luminescence measurements were further purified by chromatography on Al_2O_3 with acetone as eluent to remove minor amounts of luminescent impurities. The luminescence decay in argon-purged acetonitrile was found to be strictly monoexponential with a lifetime of 498 (20) ns. The luminescence enhancement in buffer was found to be 3000 for the Δ enantiomer with calf thymus DNA at a mixing ratio of 0.1 drug/phosphate.
(16) Barton, J. K.; Nowick, J. S. *J. Chem. Soc., Chem. Commun.* **1984**, 1650.
(17) (a) Löfroth, J.-E. Ph.D. Thesis University of Gothenburg, 1982. (b) Löfroth, J.-E. *Eur. Biophys. J.* **1985**, *13*, 45–58. (c) Eriksson, S. DNA ligand interactions studied by optical spectroscopy. Thesis, Chalmers University of Technology, Gothenburg, 1992.

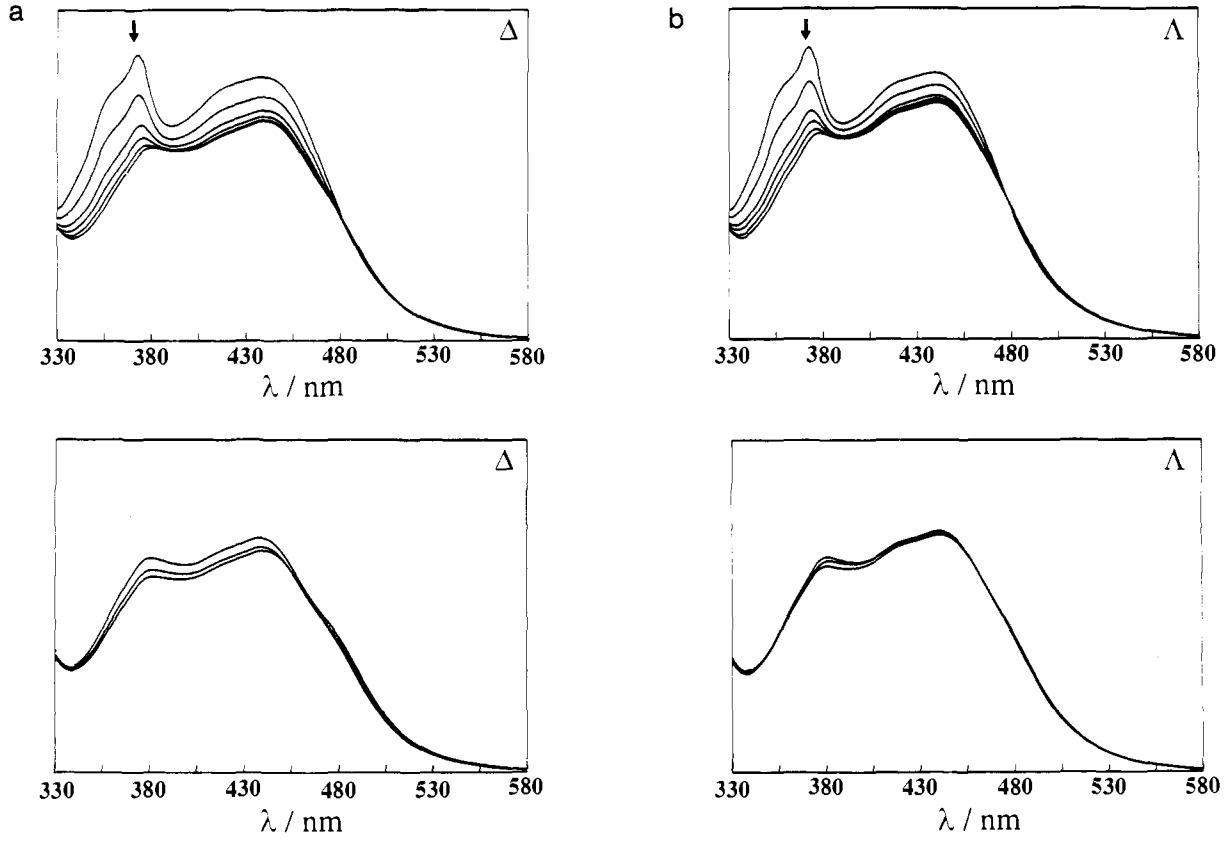

Figure 2. (a) Absorption spectra (arbitrary units) of Δ-[Ru(phen)$_2$DPPZ]Cl$_2$ in the presence of calf thymus DNA. The tail of the DNA absorption has been subtracted. The mixing ratios [metal complex]/[DNA phosphate], from the top to the bottom at 370 nm (arrow), are the following: ∞ (no DNA present), 0.83, 0.42, 0.34, 0.29, 0.25 and (lower panel) 0.06, 0.13, 0.22. (b) Absorption spectra of Λ-[Ru(phen)$_2$DPPZ]Cl$_2$, in the presence of DNA, with mixing ratios as in part a. Ru concentration was kept constant at 20 μM.

counting equipment described previously, the data being deconvoluted with the global reference method.[17a,b] The excitation wavelength was 337 nm (N_2 lamp), and emission was collected at 620 nm. Changing the excitation wavelength did not significantly affect the results; however, 337 nm was preferred since longer wavelengths required longer counting times. Isotropic absorption spectra were recorded on a Varian Cary 2300 spectrophotometer and the circular dichroism spectra on a Jasco J-500 spectrometer.

Linear Dichroism. Linear dichroism, LD, is defined as the difference in absorbance of light linearly polarized parallel and perpendicular to a macroscopic axis of orientation (the flow direction):

$$LD(\lambda) = A_{par}(\lambda) - A_{per}(\lambda) \quad (2)$$

DNA was oriented between two concentric silica cylinders in a Couette flow device,[18,19] and LD was measured on a Jasco J-500 spectrometer modified and used as described elsewhere.[20] The outer cylinder was rotated at 600 rpm, producing a flow gradient in the cell of 1800 s^{-1}. The "reduced" dichroism, LD^r, is calculated as

$$LD^r(\lambda) = LD(\lambda)/A_{iso}(\lambda) \quad (3)$$

where A_{iso} represents the absorbance of the same isotropic sample (at rest). LD^r can be factored into a product of an orientational and an optical factor:[19b]

$$[LD^r]_i = SO = \frac{3}{2}S(3\cos^2\alpha_i - 1) \quad (4)$$

where S is the orientation factor, equal to 1 for perfect orientation of the DNA helix axis parallel to the flow direction and 0 for random orientation. α_i denotes the angle between the absorbing transition moment i and the DNA helix axis. In the case of several transitions contributing to light absorption at the same wavelength, λ, the total LD is obtained as an average of the $[LD^r]_i$ weighted by the respective absorption contributions, A_i:

$$LD^r_{tot}(\lambda) = \sum [LD^r]_i A_i(\lambda) / \sum A_i(\lambda) \quad (5)$$

Results

Absorption Titration. The absorption of [Ru(phen)$_2$DPPZ]$^{2+}$ in the visible wavelength region arises from metal-to-ligand charge-transfer (MLCT) transitions (λ_{max} 439 nm) and from an intraligand (IL) transition of the DPPZ chromophore (λ_{max} 372 nm, ϵ = 21 800 M^{-1} cm^{-1}). Comparison of circular dichroism (not shown) and absorption spectra with those of the parent complex [Ru(phen)$_3$]$^{2+}$ indicates that the MLCT transitions are only slightly perturbed by the annelation of the quinoxaline moiety. Vice versa, the 372-nm IL transition appears only slightly perturbed in the metal complex as compared to the free ligand DPPZ (λ_{max} 378 nm, ϵ = 14 500 M^{-1} cm^{-1} [21]), although the intensity suggests a substantial overlap with the MLCT transitions, which will be returned to in the interpretation of the dichroism results. Figure 2 shows the behavior of the isotropic absorption spectra of the enantiomers upon interaction with DNA (constant total metal complex concentration). By increasing the DNA concentration, i.e. decreasing the mixing ratio R = [Ru]/[DNA phosphate], two phases of events with distinctly different features can be distinguished.

The top panels of Figure 2a and b represent the first phase, from free complex to R = 0.25, characterized by a hypochromic effect, which is very pronounced in the IL band. Isosbestic points are observed at 477 nm for the Λ enantiomer and at 482 nm for the Δ enantiomer. The absorption at 372 nm decreases linearly

(18) Wada, A.; Kosawa, S. *J. Polym. Sci. Part A* **1964**, *2*, 853.
(19) (a) Nordén, B.; Tjerneld, F. *Biophys. Chem.* **1976**, *4*, 191. (b) Nordén, B.; Kubista, M.; Kurucsev, T. *Q. Rev. Biophys.* **1992**, *25*, 51.
(20) (a) Davidsson, A.; Nordén, B. *Chem. Scr.* **1976**, *9*, 49. (b) Nordén, B.; Seth, S. *Appl. Spectrosc.* **1985**, *39*, 647. For a review on modulation spectroscopy with polarized light see: (c) Schellman, J. A.; Jensen, H. P. *Chem. Rev.* **1987**, *87*, 1359.
(21) Ackermann, M. N.; Interrante, L. V. *Inorg. Chem.* **1984**, *23*, 3904.

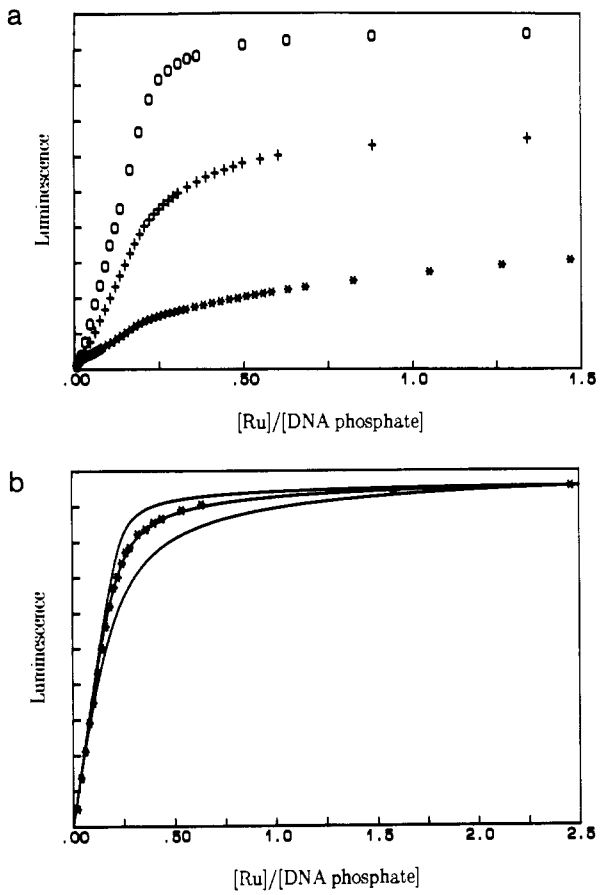

Figure 3. (a) Luminescence titration on a calf thymus DNA solution with Δ (top curve), Λ (bottom curve), and 50%Δ + 50%Λ (middle curve) enantiomers of [Ru(phen)$_2$DPPZ]Cl$_2$. Plot of corrected luminescence intensity (see Experimental) versus mixing ratio, [metal complex]/[DNA phosphate]. DNA concentration was kept constant (10 μM phosphate). λ_{exc} = 440 nm and λ_{em} = 610 nm. (b) Luminescence titration on a DNA solution (1 μM phosphate) with Δ-[Ru(phen)$_2$DPPZ]Cl$_2$ (*). Solid curves represent binding isotherms calculated according to the McGhee von Hippel equation (no cooperativity and n = 2). Curves from bottom to top correspond to K = 1.5 × 10^7, 6 × 10^7, and 2.4 × 10^8 M^{-1} and are scaled to the highest luminescence value.

with an increase in DNA concentration to R = 0.30, but to somewhat different extents for the two enantiomers. The absorption decrease of the IL band at R = 0.25 is 33% and 29% for the Δ and Λ enantiomers, respectively.

A second phase, with a different behavior is observed for mixing ratios smaller than 0.25: the absorption now increases with a decrease in mixing ratio and only a slight concomitant change of shape is observed (Figure 2, bottom panels). The effect is rather small for the Λ compared to the Δ enantiomer. From R = 0.06 to 0.005 no further change is observed for any of the enantiomers, and at these low binding ratios the absorption spectra are virtually identical for the Δ and Λ enantiomers. Compared to the spectrum of the unbound metal complex, the MLCT band exhibits no red-shift and only a moderate hypochromicity, whereas the red-shift of the IL band amounts to 8 nm. The intrinsic hypochromic effect of the IL transition is estimated at approximately 40% when the spectral overlap with the MLCT transitions is taken into account.

Luminescence Titration. Figure 3a shows the luminescence titration curves (relative luminescence intensities) for the Δ and Λ enantiomers and also for the racemate of [Ru(phen)$_2$DPPZ]$^{2+}$ at constant DNA concentration. Chromatographically purified samples of the enantiomers showed negligible luminescence in pure buffer.[15] Over a major range of binding ratios (0.08–0.20) the curves are perfectly linear, indicating that all added metal complex is bound to DNA at constant quantum yields. As calculated from the slopes of these linear parts the relative quantum yield for bound Δ complex is 5.8 times higher than that for Λ complex. The slope for the racemate is very close to the arithmetic mean of the slopes of the Δ and Λ enantiomers. The non-cooperative binding equation of McGhee and von Hippel[22] can satisfactorily be fitted to the titration data obtained for the Δ complex (Figure 3b). The best fit was obtained with the site-covering size parameter, n, equal to 2 basepairs, which corresponds to nearest-neighbor exclusion, and an intrinsic binding constant of K = 6 × 10^7 M^{-1}. Despite the excellent fit this value should be taken just as an estimate of the effective binding constant, recalling that the concentrations used are high compared to the binding constant and that the origin of the luminescence enhancement is quite complex (vide infra). In contrast to the excellent fit for the Δ enantiomer, the titration data for the Λ enantiomer are less well described by the McGhee–von Hippel equation. Importantly, however, the titration curve for the racemate coincides within 5% with the calculated arithmetic mean of the luminescence intensities observed for the separate enantiomers. We concluded that the Λ enantiomers, having a much lower quantum yield than the Δ enantiomer when bound to DNA, competes well with the Δ enantiomer for the high-affinity binding sites even when both enantiomers are present in fairly large excess. This observation demonstrates that the DNA binding constants for the Δ and Λ complexes are quite similar, i.e. there is no significant enantioselection. As seen in Figure 3a, both the Δ and Λ enantiomer curves show a marked change in curvature at $R \approx 0.25$ where binding begins to saturate. From this point to R = 1.3 the luminescence intensity is further increased by 16% and 95% for the Δ and Λ enantiomers, respectively. The substantial luminescence increase found for the Λ complex at higher ratios ($R > 0.25$) is assigned a second binding mode with lower affinity.

Excited State Lifetimes. Excited state lifetimes of Δ- and Λ-[Ru(phen)$_2$DPPZ]$^{2+}$ in the presence of calf thymus DNA, at a number of metal complex/DNA ratios, were determined using the single photon counting technique (Table I). In addition, data obtained in the presence of synthetic [poly(dA-dT)]$_2$ (AT) and [poly(dG-dC)]^2 (GC) at R = 0.1 are given in Table II. While the pure enantiomers in acetonitrile were associated with clean single-exponential decays,[15] in the presence of DNA or polynucleotide two exponentials were in all cases needed to satisfactorily fit the luminescence decays. Table III provides a comparison of steady-state luminescence intensities with intensities calculated from the time-resolved data for samples with $R \leq 0.1$, conditions under which all metal complex should be bound. The quantitative agreement is fair. It can be seen that the quantum yields decrease at very low binding ratios but that the ratio between the enantiomers is about the same. The relative quantum yield for the Δ compared to the Λ enantiomer is here about 10 for calf thymus DNA, somewhat higher than the 5.8 value estimated from the luminescence titration. In all pairs of samples having the same metal complex/DNA ratio, the most long-lived component has a substantially longer lifetime and higher relative abundancy for the Δ than for the Λ complex. This supports our conclusion from the steady state measurements that the higher luminescence intensity obtained for Δ-DNA mixtures, compared to Λ-DNA, is due to a correspondingly higher intrinsic quantum yield of the bound Δ complex. In fact, there is a fair quantitative agreement between the steady state results and the radiative quantum yields predicted from the time-resolved measurements (Table III).

For the Δ complex the longest lifetime is not significantly changed when passing from R = 0.02 to 0.25 while its relative abundancy is thereby increased from 35 to 77%. For the Λ complex the longest lifetime increases significantly while its

(22) McGhee, J. D.; von Hippel, P. H. *J. Mol. Biol.* **1974**, *86*, 469.

Table I. Luminescence Decay Parameters for Δ- and Λ-[Ru(phen)$_2$DPPZ]$^{2+}$ in the Presence of Calf Thymus DNA

	Δ enantiomer					Λ enantiomer				
R^a	$100\alpha_1{}^b$	τ_1/ns	$100\alpha_2$	τ_2/ns	$\chi^{2\,c}$	$100\alpha_1$	τ_1/ns	$100\alpha_2$	τ_2/ns	χ^2
1.0	26(11)[d]	56(29)	74(3)	516(37)	0.880	59(11)	67(14)	41(3)	391(30)	1.205
0.5	27(12)	68(37)	73(3)	588(42)	1.327	66(14)	63(14)	34(3)	362(39)	1.007
0.25	23(10)	86(46)	77(3)	649(46)	1.093	72(10)	59(8)	28(3)	287(24)	1.213
0.10	40(6)	124(3)	60(2)	699(48)	0.991	81(9)	46(5)	19(2)	233(19)	1.342
0.06	39(8)	110(29)	61(3)	680(57)	1.196	82(12)	42(6)	18(2)	232(24)	1.245
0.02	64(7)	135(16)	35(2)	733(86)	1.211	88(11)	35(2)	12(2)	192(25)	1.212
0.005	76(7)	115(10)	24(2)	439(47)	1.113	87(13)	27(4)	13(3)	116(20)	1.705

[a] Mixing ratio [ruthenium]/[DNA phosphate]. The concentration of the metal complex was 15 μM. For details, see the Experimental Section. [b] Normalized preexponential factors obtained in deconvoluting the decay curves as biexponentials. α_i reflects the proportion of component i in the luminescence at $t = 0$ (e.g. directly after the illumination). [c] Goodness-of-fit parameter, $\chi^2 = 1$ for a perfect fit. [d] Standard deviation in parentheses.

Table II. Luminescence Decay Parameters for Δ- and Λ-[Ru(phen)$_2$DPPZ]$^{2+}$ in the Presence of Various Types of DNA

	Δ enantiomer					Λ enantiomer				
type of DNA[a]	$100\alpha_1{}^b$	t_1/ns	$100\alpha_2$	t_2/ns	$\chi^{2\,c}$	$100\alpha_1$	t_1/ns	$100\alpha_2$	t_2/ns	χ^2
calf thymus	40(6)[d]	124(3)	60(2)	699(48)	0.991	81(9)	46(5)	19(2)	233(19)	1.342
AT	41(6)	134(23)	59(2)	774(55)	0.974	66(11)	42(8)	34(2)	310(22)	1.045
GC	29(7)	75(21)	71(3)	286(10)	1.083	87(9)	49(5)	13(3)	141(21)	1.183

[a] The mixing ratio [ruthenium]/[DNA phosphate] was 0.1 and the concentration of the metal complex 15 μM. For details, see the Experimental Section. [b] Normalized preexponential factors obtained in deconvoluting the decay curves as biexponentials. α_i reflects the proportion of component i in the luminescence at $t = 0$ (e.g. directly after the illumination). [c] Goodness-of-fit parameter, $\chi^2 = 1$ for a perfect fit. [d] Standard deviation in parentheses.

Table III. Relative Luminescence Intensities for Δ- and Λ-[Ru(phen)$_2$DPPZ]$_2$ in Presence of Various Types of DNA

		Δ enantiomer		Λ enantiomer		Δ/Λ enantiomer ratio	
type of DNA	R^a	RI[b]	calc[c]	RI[b]	calc[c]	RI[d]	calc[e]
AT	0.1	104	110	18	28	5.8	3.9
GC	0.1	47	48	9	13	5.1	3.7
calf thymus	0.1	=100	=100	11	18	9.1	5.7
calf thymus	0.06	97	98	9	16	10.6	6.0
calf thymus	0.02	71	73	6	12	11.9	6.4
calf thymus	0.005	44	41	5	8	8.8	4.9

[a] Mixing ratio [Ru]/[DNA phosphate]. Concentration of metal complex 15 μM. [b] Relative intensities at 620 nm, determined from steady-state emission spectra, normalized (=100) to the Δ calf thymus DNA complex ($R = 0.1$). [c] Relative intensities at 620 nm, calculated from time-resolved data in Tables I and II, according to I_{calc} proportional to $\alpha_1\tau_1 + \alpha_2\tau_2$, normalized as in footnote *b*. [d] Intensity ratio of Δ to Λ enantiomer at 620 nm determined as in footnote *b*. [e] Calculated intensity ratio of Δ to Λ enantiomer at 620 nm determined as in footnote *c*.

relative abundancy changes from 12 to 28% in the same range of ratios. However, since for each enantiomer both the lifetimes of the two components and their relative populations appear sensitive to sequence (Table II), the interpretation of this apparent ratio dependence of these parameters with the natural DNA is not straightforward. Furthermore, for Λ the excited state lifetimes and relative populations change significantly at ratios above 0.25. The population of its long life component increases significantly at the same time as its lifetime increases. These observations parallel the steady state luminescence titration results, thus supporting the existence of a second binding mode with lower affinity for the Λ enantiomer.

Linear Dichroism. Figure 4 shows flow linear dichroism spectra for DNA solutions containing either Δ- or Λ-[Ru(phen)$_2$DPPZ]$^{2+}$. The absorption in the long-wavelength region of the spectrum (>300 nm) is due solely to transitions in the metal complex. The non-zero LD in this region is therefore a direct visualization of those metal complex ions that are non-randomly oriented by association to DNA. From the signs and amplitudes of the LD signals geometric information about the binding mode is provided: positive LD implies that a transition has its transition moment more parallel to the DNA helix axis, and negative LD corresponds to a more perpendicular orientation. Exact angles of orientation can be determined from eqs 4 and 5 once the degree of orientation (S) and the extent of overlap between different transitions are known (see below).

The shapes of the LD spectra in the visible region are very similar for the Δ and Λ enantiomers, indicating quite similar binding geometries upon complexation to DNA for the two enantiomers. An essentially constant spectral shape of the LD contribution from bound metal complex, evidenced by isodichroic points in the UV region and fixed points where the LD spectra cross the zero-line in the visible region, indicates that the metal complex has by large the same orientation on DNA at low and high binding ratios.

In the UV region, the LD amplitude varies considerably upon binding of [Ru(phen)$_2$DPPZ]$^{2+}$ to DNA. This effect was found to be due to changed DNA orientation. When the Λ complex is added an *increase* of the LD in the DNA base absorption region is observed, suggesting that this enantiomer enhances the orientation (increased orientation factor S), i.e. that it stiffens DNA. With the Δ enantiomer it is not immediately apparent whether the DNA orientation is changed. Using an iterative procedure described before,[6a] S can be calculated via the metal complex LD, at the assumption of a fixed binding geometry. We found that when going from $R = 0$ (pure DNA) to 0.20, S is almost doubled for the Λ enantiomer, whereas it increases only some 25% for the Δ enantiomer. Furthermore, subtraction of the intrinsic DNA dichroism (scaled to correct amplitude using the calculated S values) yielded LD spectra in the UV region for the contribution from metal complex which were very similar for the Δ and Λ enantiomers, again indicating similar DNA binding geometries for the two complexes (results not shown).

When the titration is carried beyond $r = 0.25$, the amplitudes of the LD curves, both in UV and visible, begin to scale down. This decrease of S is most likely an effect of compaction and/or aggregation as a result of the neutralization of the DNA phosphate charges.

In order to determine binding geometry we need first to assign transitions and transition moment directions of the metal complex chromophores. The LD spectra of the DNA adducts with both enantiomers contain three main features above 300 nm: one negative peak at 480 nm, a broad positive band centered at 425 nm, and a structured negative band between 300 and 380 nm. From LD measurements on the complex oriented in stretched poly(vinyl alcohol) films it is concluded that the latter (372 nm) band is due to a $\pi \rightarrow \pi^*$ transition polarized along the long axis

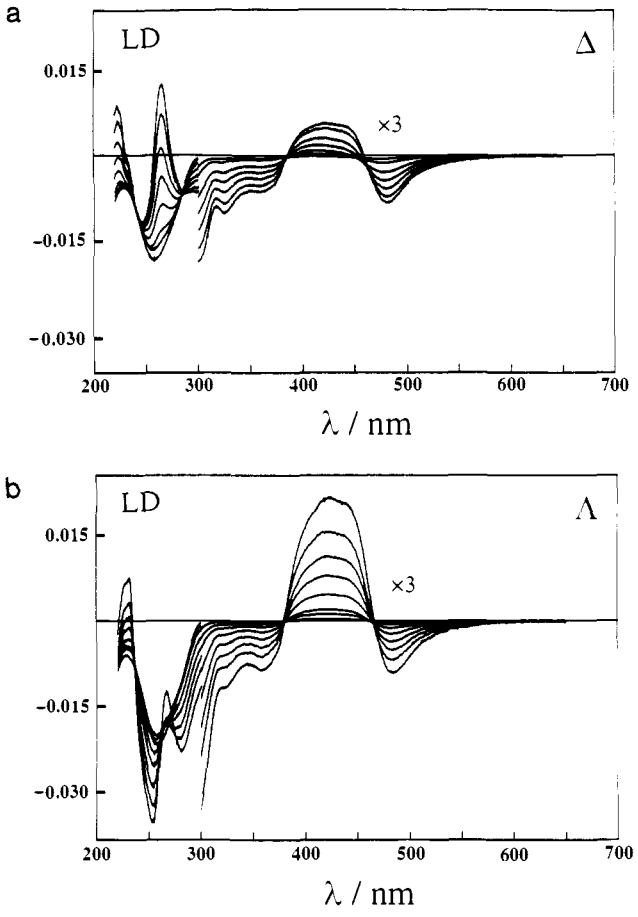

Figure 4. Linear dichroism (LD) spectra of flow-oriented calf thymus DNA solution containing $[Ru(phen)_2DPPZ]Cl_2$: (a) Δ enantiomer, (b) Λ enantiomer. Mixing ratio [metal complex]/[DNA phosphate] from the bottom to the top at 425 nm: 0 (pure DNA), 0.012, 0.030, 0.059, 0.089, 0.118, 0.148, 0.177 for the Δ enantiomer (a), and 0 (pure DNA), 0.006, 0.030, 0.061, 0.091, 0.122, 0.152, 0.213 for the Λ enantiomer (b). At 250 nm, the order of appearance of the curves is the same as given for the Δ enantiomer whereas it is reversed for the Λ enantiomer. The DNA concentration is 0.25 mM phosphate. LD intensity (in absorbance units) is normalized to 1 cm optical path length.

of the DPPZ ligand.[23] Unfortunately this band is overlapped by the positive MLCT band on its low-energy side which prevents exact determination of the $[LD^r]_i$ value for the DPPZ transition and its α value. At $R = 0.075$ the optical factor of eq 4 (LD^r/S) is –0.59 for the Δ enantiomer and –0.47 for the Λ enantiomer. Using eq 4 a lower limit of the angle between the molecular long axis of the DPPZ wing and the DNA helix axis is calculated to be 62 ± 1° for both enantiomers from the measured LD^r values. However, as judged from the absorption curves (Figure 2) and by comparison with the spectra of pure DPPZ ligand and of $[Ru(phen)_3]^{2+}$,[6a] the overlap from the MLCT band is extensive: it is estimated to contribute about 50% of the total absorption at 380 nm. If $[LD^r]^i$ for the MLCT transition is assumed to lie between ±0 and +0.9 (the LD^r/S maximum at 450 nm), the $[LD^r]_i$ for the DPPZ transition is according to eq 5 between –1.2 and –1.4, i.e. α = 70–80°. These angles are consistent with orientations for Δ- and Λ-[Ru(phen)DPPZ]²⁺ in which the molecular plane of the DPPZ wing is essentially parallel to the plane of the DNA bases.[19b]

Discussion

An important finding of this study is the large difference in luminescence quantum yields between the enantiomeric forms of $[Ru(phen)_2DPPZ]^{2+}$ upon binding to DNA. Since the time-resolved luminescence reveals a complex picture, it is relevant to first consider any evidence for different binding modes that the various spectroscopic techniques may provide.

Binding Geometry. The LD data provide solid support for an intercalative binding mode. The IL absorption band corresponding to a transition polarized in the plane of the DPPZ wing exhibits an LD that suggests both Δ- and Λ-$[Ru(phen)_2DDPZ]^{2+}$ be bound with the DPPZ ligand nearly perpendicular to the DNA helix. Significant differences between the LD spectra in the MLCT region indicate that the binding geometry varies somewhat between the enantiomers, which can be related to the fact that the dissymmetric pair of non-intercalated phenanthroline ligands interacts differently with the helical DNA strands surrounding the groove in which the complex sits. The increase in orientation factor S, indicating an increased persistence length of DNA, is also an observation consistent with intercalation. The pronounced hypochromicity and the red-shift in the IL $\pi \rightarrow \pi^*$ transition of the DPPZ chromophore are typical for stacking interactions with the base pairs.

Intercalation is further supported by the high affinity found from the luminescence titration with effective binding constants $K_{eff} \approx 10^8$ M^{-1} and the value of the site size parameter $n = 2$ which corresponds to nearest-neighbor exclusion. However, it should again be noted that the determination is only a rather crude estimate of the binding constant due to the nonlinear response at very low binding ratios and the high overall concentrations in the titration. Nevertheless, the binding affinity is several orders of magnitude larger than for the parent compound, $[Ru(phen)_3]^{2+}$, in accord with the increased possibility for hydrophobic interactions between the extended π-system of the DPPZ ligand and the DNA base pairs. The binding parameters could be compared with another high-affinity binding ruthenium complex possessing an extended polycyclic ligand, $[Ru(phen)_2$-(9,10-phenanthrenequinonediimine)$]^{2+}$, which has $K = 10^5$ M^{-1} and $n = 2$–3 in buffered 50 mM NaCl.[24] The high binding density attainable for these rather bulky complexes is remarkable and suggests that the packing of the non-intercalating phenanthroline ligands for contiguously bound complexes could be an additional diastereomeric factor influencing the properties of the system.

A second important result from the LD measurements is that each enantiomer shows only one binding geometry up to a binding ratio of about 0.2. The unchanged shape of the LD spectra at long wavelengths and the isodichroic points in the UV region could either mean that the metal complexes bind with a single binding geometry or, in case they exhibit multiple binding modes with different distinct binding geometries, that these occur in the same proportions throughout the titration. The latter alternative, however, is unlikely since it would require identically high binding constants for geometrically different binding modes.

Enantiospecific Luminescence. The luminescence of $[Ru(L)_2DPPZ]^{2+}$ is believed to be related to a delocalized charge-transfer excitation preferentially trapped on the DPPZ ligand so that an excited state dipyridophenazine anion radical is created.[3] In aqueous solution the luminescence is efficiently quenched, probably by protonation of the phenazine nitrogen by water.[3] The enhancement in emission and the corresponding increase of excited state lifetimes observed upon binding of $[Ru(phen)_2$-$DPPZ]^{2+}$ to DNA thus reflect an efficient protection of the DPPZ excited state radical from solvent water.[2a] Such protection demands embedding of the phenazine moiety of the DPPZ ligand deep into the DNA helix which is achieved when it is sandwiched between base pairs.

The steady state as well as time-resolved luminescence data clearly show that it is mainly the Δ enantiomer that is responsible for the luminescence enhancement recently reported for racemic $[Ru(phen)_2DPPZ]^{2+}$ upon binding to double-helical B-form

(23) Lincoln, P.; Hiort, C.; Nordén, B. To be published.

(24) Pyle, A. M.; Rehmann, J. P.; Meshoyrer, R.; Kumar, C. V.; Turro, N. J.; Barton, J. K. *J. Am. Chem. Soc.* **1989**, *111*, 3051.

DNA.[25] This behavior is obviously not a result of different affinities of the enantiomers for DNA or to radically different binding geometries. Barton and co-workers have reported biexponential decays for interaction of the racemate with various DNAs;[25] however, we show here that each enantiomer when bound has two distinct lifetimes. At first glance it might therefore seem as if the time-resolved luminescence data and the absorption titration data were in conflict with the conclusion from LD about a single binding geometry. The two lifetimes found for each enantiomer must be interpreted in terms of, at least, two different excited species contributing to the emission. Importantly, however, in a wide range of ratios ($0.005 < R < 0.25$) the amplitudes of these components change considerably with binding ratio for both enantiomers, which would lead to changes in the total LD spectra if their binding geometries were different. Since such changes are not observed we suggest that the excited species instead differ only in respect to their environment, for example, by being bound within a contiguous sequence of metal complexes or dependent on base pair sequence. We observe that the amplitudes of the long-lived species increase with increasing degree of occupancy up to the saturation limit ($R \approx 0.25$), suggesting that the distribution of metal complexes on DNA is an important factor. The long lifetime may originate from sequences of closely bound intercalators and the short lifetime from more or less isolated intercalating complexes. The relative abundancies as well as the lifetimes are also dependent on the type of DNA (Table II). However, since two distinct lifetimes are observed also in $[poly(dA\text{-}dT)]_2$ and $[poly(dG\text{-}dC)]_2$, sequence heterogeneity seems not to be a main origin of the observed different luminescent species. Further support for the interaction between closely bound metal complexes is the extra hypochromic effect observed in absorption as the binding density is increased from $R = 0.06$ to 0.25. Interestingly, this effect is more pronounced for the Δ than for the Λ enantiomer, in parallel with the greater abundance of the long-lived component in the Δ enantiomer titration. One may thus speculate that a longer lived excited state is an effect of close packing providing a more efficient barrier to quenching water than for isolated complex units.

The time-resolved data show that both the relative populations of the long-lived and the short-lived components and their lifetimes are responsible for the lower quantum yield of the Λ enantiomer (Table I). Thus, the difference in quantum yield appears to emanate from a minor difference in binding geometry as well as differences in the interactions between closely bound complexes resulting in different exposure to solvent water for the DPPZ ligand of the two enantiomers.

External Binding. At high metal complex/DNA mixing ratios ($R > 0.25$) DNA is almost saturated with respect to the intercalative binding mode and, as is indicated by the absorption titration, free metal complex is present in the solution. At these high ratios, we observe a substantial steady-state luminescence increase and a corresponding increase in amplitude and lifetime of the long-lived component in the time-resolved measurements for enantiomer Λ (Table I). As indicated by the titration for the racemate, this is not due to a lower binding constant of enantiomer Λ for the intercalation site. Instead, this observation suggests a second binding mode of lower affinity for enantiomer Λ to DNA. This type of binding may be the unspecific electrostatic outer-sphere binding that occurs to any polyelectrolyte. The luminescence increase could be due to the fact that the DPPZ ligands of the metal complexes in the low affinity site are somewhat shielded from water. However, another possibility is that these outer complexes provide further shielding for metal complexes bound in intercalation sites.

Racemic Studies. Since the first preliminary report of our results was given,[2d] two papers by Barton and co-workers[25] have appeared reporting luminescence data on racemic $[Ru(phen)_2DPPZ]^{2+}$ in the presence of DNA. Their time-resolved results are analyzed in terms of biexponential decays. It appears that the long-lived Δ component is reasonably resolved, and in good agreement with our results, but that the other three components are averaged into a shorter apparent lifetime in the racemate. To account for the two species the authors proposed two different intercalative orientations, based on the observation of three lifetimes for a racemic complex with an unsymmetrically substituted DPPZ ligand. Although the latter argument is invalidated by our observation of the quite different luminescence properties for the two enantiomers of the parent complex, the two speculated binding geometries are interesting regarding the diastereomeric differences that we note for the intercalated complexes. It should be noted that LD alone (in contrast to induced CD)[19b] cannot discriminate between binding geometries that are related by a rotation around the DNA helix axis. However, it is reasonable that different intercalative orientations would be highly sensitive to the diastereomeric interactions of the phenanthroline ligands with the walls of the groove.

Conclusions

The following have been learnt from this study:

1. Pure enantiomers of the complex $[Ru(phen)_2DPPZ]^{2+}$ have been synthesized.
2. The Δ enantiomer is by an order of magnitude higher quantum yield primarily responsible for the luminescence enhancement upon DNA binding previously reported for the racemate. The steady state results have quantitative support from the time-resolved luminescence decay data.
3. Each of the enantiomers shows a biexponential luminescence decay upon binding to DNA (implying four distinct lifetimes for the racemate).
4. Both enantiomers bind extremely strongly to DNA ($K = 10^8\ M^{-1}$) but without any noticeable enantioselectivity. A limiting binding ratio of 0.25 indicates an efficient packing of these rather bulky DNA ligands.
5. The angular orientation of the DPPZ ligand, as judged from linear dichroism spectroscopy, indicates that both the Δ and the Λ complexes bind by intercalation of this elongated planar moiety between the DNA base pairs.
6. A slight difference in binding geometry is observed between the enantiomers. However, for each enantiomer the same geometry holds up to high (0.2) binding ratios.
7. The distribution of the metal complexes on DNA is of importance for the spectroscopic properties. Closely bound metal complexes give rise to extra hypochromicity in the absorption and further enhanced luminescence.
8. We propose that the pronounced difference in quantum yield between the enantiomers is due to a certain difference in location of the DPPZ ligand within the intercalation pocket but that also interactions between closely bound complex ions may play a role.

Acknowledgment. Dr. Kjell Sandros is gratefully acknowledged for valuable discussions and for conducting the time-resolved measurements. This project is supported by the Swedish Natural Science Research Council.

(25) (a) Hartshorn, R. M.; Barton, J. K. *J. Am. Chem. Soc.* **1992**, *114*, 5919. (b) Jenkins, Y.; Friedman, A. E.; Turro, N. J.; Barton, J. K. *Biochemistry* **1992**, *31*, 10809.